

QUANTIFYING REGIONAL GROWTH PATTERNS THROUGH LONGITUDINAL ANALYSIS OF DISTANCES BETWEEN MULTIMODAL MR INTENSITY DISTRIBUTIONS

Avantika Vardhan¹, Marcel Prastawa¹, Sylvain Gouttard¹, Joseph Piven² for IBIS*, Guido Gerig¹

¹Scientific Computing and Imaging Institute
University of Utah
Salt Lake City, UT 84112

²Department of Psychiatry
University of North Carolina
Chapel Hill, NC 27599

ABSTRACT

Quantitative analysis of early brain development through imaging is critical for identifying pathological development, which may in turn affect treatment procedures. We propose a framework for analyzing spatiotemporal patterns of brain maturation by quantifying intensity changes in longitudinal MR images. We use a measure of divergence between a pair of intensity distributions to study the changes that occur within specific regions, as well as between a pair of anatomical regions, over time. The change within a specific region is measured as the contrast between white matter and gray matter tissue belonging to that region. The change between a pair of regions is measured as the divergence between regional image appearances, summed over all tissue classes. We use kernel regression to integrate the temporal information across different subjects in a consistent manner. We applied our method on multimodal MRI data with T1-weighted (T1W) and T2-weighted (T2W) scans of each subject at the approximate ages of 6 months, 12 months, and 24 months. The results demonstrate that brain maturation begins at posterior regions and that frontal regions develop later, which matches previously published histological, qualitative and morphometric studies. Our multimodal analysis also confirms that T1W and T2W modalities capture different properties of the maturation process, a phenomena referred to as T2 time lag compared to T1. The proposed method has potential for analyzing regional growth patterns across different populations and for isolating specific growth critical maturation phases in different MR modalities.

Index Terms— Early brain development, structural MRI, longitudinal analysis, distribution statistics, MR contrast analysis

1. INTRODUCTION

The brain undergoes far more significant changes with respect to shape, structure, size, and chemical composition between birth and two years than at any other stage [1]. Quantifying these changes at this critical stage of development is clinically relevant for analyzing

This work is supported by NIH grants ACE RO1 HD 055741, Twin R01 MH070890, and Conte Center MH064065. *The IBIS Network. Clinical Sites: University of North Carolina: J. Piven (IBIS Network PI), H.C. Hazlett, C. Chappell; University of Washington: S. Dager, A. Estes, D. Shaw; Washington University: K. Botteron, R. McKinstry, J. Constantino, J. Pruett; Childrens Hospital of Philadelphia: R. Schultz, S. Paterson; University of Alberta: L. Zwaigenbaum; Data Coordinating Center: Montreal Neurological Institute: A.C. Evans, D.L. Collins, G.B. Pike, P. Kostopoulos; Samir Das; Image Processing Core: University of Utah: G. Gerig; University of North Carolina: M. Styner; Statistical Analysis Core: University of North Carolina: H. Gu; Genetics Analysis Core: University of North Carolina: P. Sullivan, F. Wright.

normal and pathological development, and can provide information about effective clinical intervention and management procedures. The processes which take place during the early development of the brain, such as premyelination, myelination, axonal pruning, and water compartmentalization, are highly region-specific [2]. Growth and maturation of different cortical regions are therefore known to be heterogeneous [1, 3]. Myelination is the creation of a lipid myelin bilayer around neuronal axons which alters the properties of water in brain tissue. This process in turn leads to changes in the longitudinal and transverse relaxation times which are measured in T1-weighted (T1W) and T2-weighted (T2W) MR images respectively. The progression of myelination from posterior regions of the brain, such as the parietal and occipital lobes, to anterior regions, such as the temporal and frontal lobes, has been studied by visual inspection of MRI [1] and with the use of specialized MR sequences [2]. Fig. 1 shows spatially registered, longitudinal MR scans of an infant with changes due to myelination, cortical folding, and variations in biophysical properties, along with the parcellation atlas used to extract each lobar region.

Quantitative studies of longitudinal MR images have demonstrated change of morphometric properties such as volumes of brain tissues and cortical thickness [3, 4]. However, only a few quantitative studies have analyzed the temporal variations seen in the signal intensity of MRI [5, 6, 7]. In a recent study, Serag et al. [5] performed a kernel regression based cross-sectional analysis on MR images of premature infants to track spatiotemporal changes in MR intensity. Sadeghi et al. [6] used the Gompertz function to model time varying intensities and characterize white matter maturation. Aljabar et al. [7] focused on modeling both shape as well as appearance but did not quantify temporal changes in regional contrast and inter-region variations in appearance.

Similar to [5], we seek to characterize the trajectory of brain growth and maturation by quantifying changes in the intensity and contrast of Magnetic Resonance (MR) images. We propose a framework to measure differences between intensity distributions across brain regions, ages and modalities using divergence measures. Temporal analysis of these differences is performed through the use of kernel regression to obtain consistent spatiotemporal measures of growth over time. Our new method is applied to image data taken from longitudinal structural MR imaging study of infants from age 6 months to 2 years for analysis of temporal changes in the occipital, temporal, frontal, and parietal lobes.

2. METHOD

We use a subset of the longitudinal dataset from the Infant Brain Imaging Study of the University of North Carolina Autism Cen-

ter for Excellence (ACE-IBIS) project. The dataset used consists of scans of 10 subjects with three repeated scans acquired at 6-9 months, 12-15 months, and 24-28 months of age. Each scan consists of T1W and T2W structural modalities, which results in a total of 60 images used in our analysis.

In order to analyze properties of the intensity distributions, we standardize each image to a common reference space, hence removing shape and size differences. This is done using a localized, free form deformation method based on B-splines, which uses normalized mutual information as the metric for image matching [8]. This is followed by applying an image segmentation method that uses the segmentation map of a 2 year old as a prior for segmenting the 6 month and 12 month old MR scans [9]. Images are preprocessed for bias inhomogeneity by using the N3 algorithm [10], which adopts a nonparametric approach to estimate true tissue intensity values in the presence of a multiplicative bias field. We remove variations in the intensity ranges of images by performing intensity normalization on the entire dataset. The intensity values of each image are normalized using a multiplicative factor which was obtained by computing the median value of manually segmented regions of fatty tissue and ventricular cerebrospinal fluid (CSF), in the T1W and T2W scans respectively. Fig. 1 shows the spatially registered and intensity-normalized longitudinal MR scans of one infant, clearly demonstrating the changes due to myelination and variations in biophysical properties, along with the parcellation atlas used to extract each lobar region.

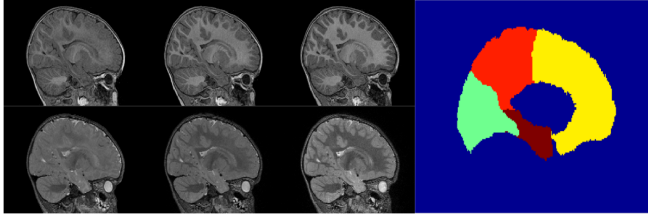


Fig. 1. T1W (top) and T2W (bottom) MR images scanned at age 6, 12, and 24 months (from left to right). Lobar regions are shown as a color image on the right (Occipital = cyan, Temporal = brown, Frontal = yellow, Parietal = orange).

2.1. Distance Metric between Intensity Distributions

We use the Hellinger distance (HD) as the basis of our measurements. The Hellinger distance is a divergence measure between two probability distributions that is derived from the Bhattacharyya coefficient (BC). It satisfies the properties of a metric and is hence applied instead of measures such as the Kullback-Leibler divergence or the Bhattacharyya distance. It has been successfully used in several statistical applications and does not require the underlying distribution to be in a specific form. Given two probability distributions $m(x)$ and $n(x)$, the Bhattacharyya coefficient between them is defined as an integral over the range of x , given by: $BC(m, n) = \int \sqrt{m(x)n(x)}dx$. This gives rise to the Hellinger distance between m and n , defined according to [11] as:

$$HD(m, n) = \sqrt{2(1 - BC(m, n))} \quad (1)$$

Following this definition, it can be seen that the Hellinger distance is bounded as $HD \in (0, \sqrt{2})$. For a particular modality, each subject s is imaged at 3 discrete time points $\{t_{s,1}, t_{s,2}, t_{s,3}\}$, giving rise to

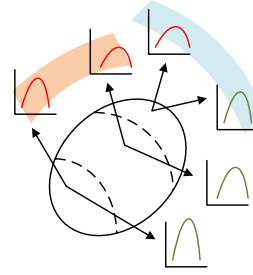


Figure 2. Overview of the distances between distributions used in our analysis, Class 1 and Class 2 are given by the red curve and green curve respectively. Distances are shown within a region between two classes (light blue band), and between a pair of regions (orange band).

a tuple of probability distribution functions given by:

$$P_{R_i, s, c} = \left(P_{R_i, s, c}^{t_{s,1}}, P_{R_i, s, c}^{t_{s,2}}, P_{R_i, s, c}^{t_{s,3}} \right) \quad (2)$$

for a region of interest $R_i \in \{Occipital, Temporal, Frontal, Parietal\}$ and tissue class $c \in \{white-matter, gray-matter\}$. Thus, the Hellinger distance at a time point $t_{s,k}$, between a pair of intensity distributions is written as

$$HD_{t_{s,k}} \left(P_{R_i, s, c_a}^{t_{s,k}}, P_{R_j, s, c_b}^{t_{s,k}} \right). \quad (3)$$

A conceptual overview of two cases involving this distance is given in Fig. 2. They are outlined as:

1. $R_i = R_j = R$ and $c_a \neq c_b$, where the distance gives us the contrast between classes c_a, c_b in a region R at a time point $t_{s,k}$, measured as,

$$HD_{t_{s,k}} \left(P_{R, s, c_a}^{t_{s,k}}, P_{R, s, c_b}^{t_{s,k}} \right). \quad (4)$$

2. $R_i \neq R_j$ and $c_a = c_b = c$, where the distance gives us the regional differences of a class c between the regions R_i, R_j at a time point $t_{s,k}$ measured as

$$HD_{t_{s,k}} \left(P_{R_i, s, c}^{t_{s,k}}, P_{R_j, s, c}^{t_{s,k}} \right). \quad (5)$$

2.2. Longitudinal Analysis of Distances

As we are analyzing longitudinal data, we are interested in determining how these distances vary as a function of time. We perform kernel regression on the distances between distributions to measure these variations. At time t , the distance between classes c_a and c_b across all subjects is measured as

$$D_{R, c_a, c_b}(t) = \int_s \frac{\sum_{t_{s,k}} K(t, t_{s,k}) HD_{t_{s,k}} \left(P_{R, s, c_a}^{t_{s,k}}, P_{R, s, c_b}^{t_{s,k}} \right)}{\sum_{t_{s,k}} K(t, t_{s,k})} ds \quad (6)$$

Similarly, at time t , the distance between regions R_i and R_j across all subjects is measured as

$$D_{R_i, R_j}(t) = \int_s \frac{\sum_{t_{s,k}} K(t, t_{s,k}) \sum_c HD_{t_{s,k}} \left(P_{R_i, s, c}^{t_{s,k}}, P_{R_j, s, c}^{t_{s,k}} \right)}{\sum_{t_{s,k}} K(t, t_{s,k})} ds \quad (7)$$

where $t_{s,k}$ denotes the observed time points of scans specific to the subject s , and $K(\cdot, \cdot)$ denotes a kernel function which is chosen to be

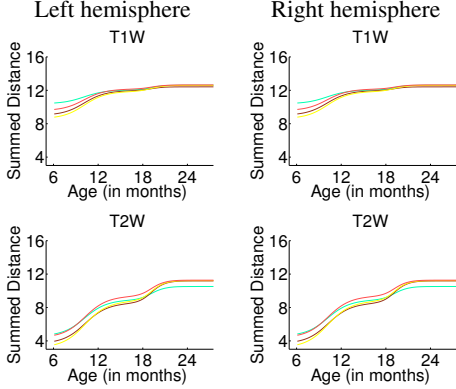


Figure 4. Distance function $D_{R,c_a,c_b}(t)$ measuring contrast for lobes: Occipital (cyan), Temporal (brown), Frontal (yellow), Parietal (orange).

a Gaussian kernel in all our subsequent analysis. Different modalities (T1W and T2W) display varying trajectories of contrast change, since they capture different biophysical properties involved in brain development. To quantify the differences in time taken for each modality to reach adult-like image contrast, we define τ as the earliest time taken to reach 90 percentage of the maximum contrast, a monotonically increasing function which reaches a maximum value at 24 months or time t_{max} . More specifically,

$$\tau = \min_t D_{R,c_a,c_b}(t) \geq 0.9 D_{R,c_a,c_b}(t_{max}) \quad (8)$$

3. RESULTS

We perform analysis of the different lobes in the left and right hemispheres separately to preserve possible asymmetry in growth patterns. The changes in the intensity distributions of one subject are shown in Fig. 3. As seen in the figure, contrast between white and gray matter tends to increase with time while the distances between distributions at different lobes tend to stabilize. T1W and T2W modalities also show dissimilar progression of changes.

Changing contrast (Eq. 6) at each lobe is illustrated in Fig. 4. Contrast is measured between white matter and gray matter, as their variations are of major concern compared to those of other structures such as cerebrospinal fluid. The overall trend is for the contrast to increase over time, though the progression differs for T1W and T2W at the left and right hemispheres. This increase is also non-uniform, with the greatest changes occurring between 6 and 12 months, particularly in T1W images while T2W images continue to undergo significant change up to 2 years of age. Unlike T1W images, T2W images show little contrast at 6 months.

We show the difference between pairs of regions (Eq. 7) in Fig. 5. At 6 months, the distance between occipital and all other lobes is the largest since at this stage it has undergone myelination while the other lobes have not. The distance between parietal and frontal lobes in T1W images is small at 24 months which confirms previous studies stating that these regions are highly similar at this age. The distances between regions in T2W images follows two patterns: decreasing or increasing with time. The increasing pattern occurs most clearly in the comparisons between occipital and other lobes, where we observe significant increase after 12 months, related to the early development of the occipital lobe. The difference of growth patterns between T1W and T2W is likely caused by the fact that the first phase of growth is not captured by the T2W modality at 6 months which results in low T2W contrast [1], and the distance increases at 12 months during the second growth cycle.

Occipital		Temporal		Frontal		Parietal	
T1	T2	T1	T2	T1	T2	T1	T2
11.3	17.1	11.3	19.5	11.3	18.9	11.3	15.5
11.1	18.3	11.3	18.5	11.7	18.9	9.9	16.7
15.5	19.1	13.3	19.5	17.1	19.5	13.7	19.3
6.1	18.9	9.1	19.3	12.3	18.9	6.1	18.7
6.1	16.9	11.5	19.5	11.7	19.5	10.7	19.3
10.3	19.5	13.3	19.9	14.5	19.9	12.5	19.5
12.3	17.5	12.3	19.9	15.9	19.7	12.5	19.3
6.1	20.7	7.9	21.1	12.3	21.1	9.1	20.7
11.1	16.3	10.9	17.3	11.7	18.9	10.9	14.7
6.1	18.7	9.1	19.5	11.1	19.5	8.7	19.5

Table 1. τ of 10 subjects for right hemisphere T1W, T2W scans.

We list the values of τ in Table. 1, that quantifies the different progressions of the image contrast changes for T1W and T2W in the right hemisphere. The τ values for T1W are consistently lower than the ones for T2W across all regions showing that image contrast develops later for T2W modalities. The measured values of τ show a similar trend in the left hemisphere, thereby indicating that these modalities capture different characteristics of the growth process.

4. CONCLUSIONS

We have presented a framework for comparing growth patterns by measuring distances between brain tissue intensity distributions on intensity-normalized image data. We have defined a distance between spatial regions, and a distance that measures image contrast of different tissue categories within one region. Longitudinal analysis of these distance values via kernel regression yields observations that conform with results from previous imaging studies [1, 2].

The results demonstrate that brain maturation begins at posterior regions while frontal regions develop later, as previously established in both qualitative and morphometric studies. Our multimodal analysis also shows that T1W and T2W modalities capture different properties of the maturation process, where the T2 changes seem to lag behind the more rapid T1 changes. Further, the proposed method has potential for isolating specific critical phases of maturation, which might better explain a correlation between imaging findings and cognitive assessments.

In the future, we will explore alternatives to kernel regression which are more suited to longitudinal data to avoid the staircasing artifacts. Whereas this feasibility study was using a random selection of subjects from an ongoing autism study, we will focus on a statistical analysis of differences in growth trajectories between healthy subjects and those at risk for autism. We will consider application to other longitudinal infant studies to determine differences between healthy populations and subjects with mental illness or neurological disorders, and to detect longitudinal trajectories of pathological patterns associated with cognitive and behavioral differences.

5. REFERENCES

- [1] Mary Rutherford, *MRI of the Neonatal Brain*, W.B. Saunders, 2002.
- [2] S. C. Deoni, E. Mercure, A. Blasi, D. Gasston, A. Thomson, M. Johnson, S. C. Williams, and D. G. Murphy, "Mapping infant brain myelination with magnetic resonance imaging." *J. Neurosci.*, vol. 31, pp. 784–791, Jan 2011.

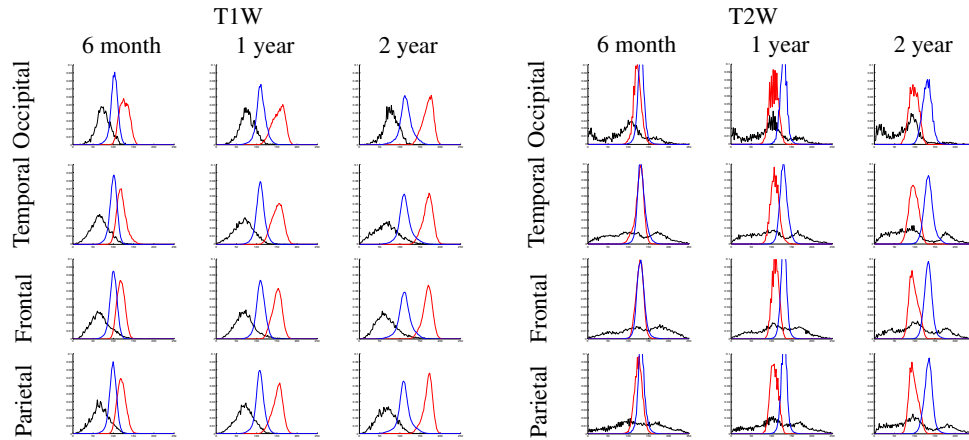


Fig. 3. T1W and T2W intensity distributions for a chosen subject in the major lobes of the right hemisphere. The WM, GM, and CSF distributions are represented by red, blue, and black curves respectively. The area under each curve is normalized to unity.

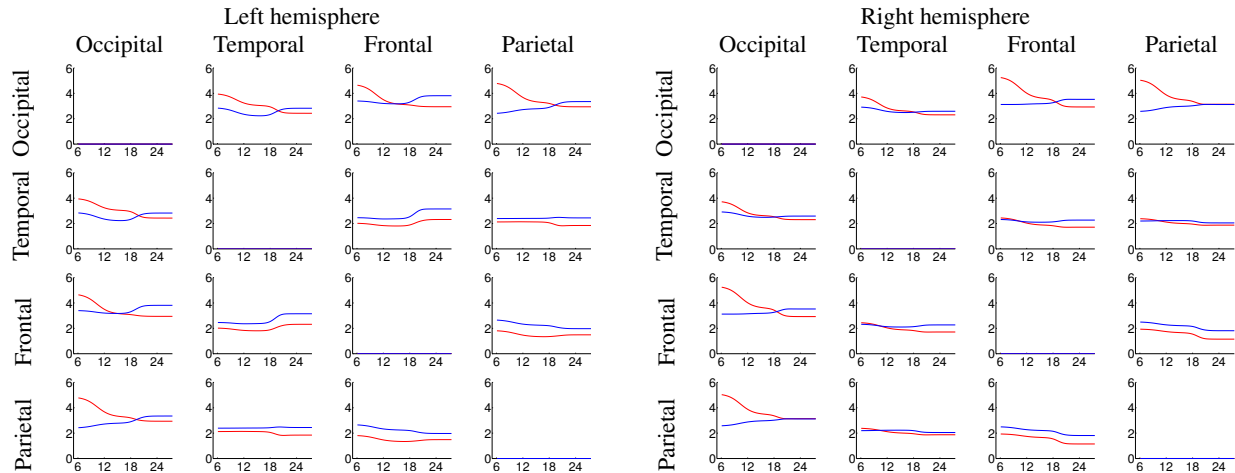


Fig. 5. Distance between regions of the left and right hemispheres across time, for T1W (red) and T2W (blue) modalities. For each figure, the vertical axis represents distance summed over all subject, the horizontal axis gives age in months.

- [3] J. N. Giedd, J. Blumenthal, N. O. Jeffries, F. X. Castellanos, H. Liu, A. Zijdenbos, T. Paus, A. C. Evans, and J. L. Rapoport, "Brain development during childhood and adolescence: a longitudinal MRI study," *Nat. Neurosci.*, vol. 2, Oct 1999.
- [4] P. Aljabar, K. K. Bhatia, M. Murgasova, J. V. Hajnal, J. P. Boardman, L. Srinivasan, M. A. Rutherford, L. E. Dyet, A. D. Edwards, and D. Rueckert, "Assessment of brain growth in early childhood using deformation-based morphometry," *Neuroimage*, vol. 39, pp. 348–358, Jan 2008.
- [5] A. Serag, P. Aljabar, S. Counsell, J.P. Boardman, J.V. Hajnal, and D. Rueckert, "Tracking developmental changes in subcortical structures of the preterm brain using multi-modal MRI," in *Proc. ISBI*, 2011, pp. 349–352.
- [6] N. Sadeghi, M. Prastawa, J.H. Gilmore, W. Lin, and G. Gerig, "Spatio-temporal analysis of early brain development," in *Proceedings IEEE Asilomar Conference on Signals, Systems and Computers*. IEEE, 2010.
- [7] P. Aljabar, R. Wolz, L. Srinivasan, S.J. Counsell, M.A. Rutherford, A.D. Edwards, J.V. Hajnal, and D. Rueckert, "A combined manifold learning analysis of shape and appearance to characterize neonatal brain development," *Medical Imaging, IEEE Transactions on*, vol. 30, pp. 2072–2086, dec. 2011.
- [8] D. Rueckert, L. I. Sonoda, C. Hayes, D. L. Hill, M. O. Leach, and D. J. Hawkes, "Nonrigid registration using free-form deformations: application to breast MR images," *IEEE Trans Med Imaging*, vol. 18, pp. 712–721, Aug 1999.
- [9] Sun Hyung Kim, V. Fonov, J. Piven, J. Gilmore, C. Vachet, G. Gerig, D.L. Collins, and M. Styner, "Spatial intensity prior correction for tissue segmentation in the developing human brain," in *Proc. ISBI*, 2011, pp. 2049–2052.
- [10] J.G. Sled, A.P. Zijdenbos, and A.C. Evans, "A nonparametric method for automatic correction of intensity nonuniformity in MRI data," *IEEE Trans Med Imaging*, vol. 17, pp. 87–97, 1998.
- [11] Alison L. Gibbs and Francis Edward Su, "On choosing and bounding probability metrics," *International Statistical Review*, vol. 70, no. 3, pp. 419–435, Jan 2002.